

Is nonstandard interaction a solution to the three neutrino tensions?

Shinya Fukasawa,^{*} Monojit Ghosh,[†] and Osamu Yasuda[‡]

Department of Physics, Tokyo Metropolitan University, Hachioji, Tokyo 192-0397, Japan

In this work we present a scenario in which a nonstandard interaction in neutrino propagation can explain the three major tensions in the neutrino oscillation data at present. These tensions are: (i) a non-zero best-fit value of the non-standard oscillation parameters in the the global analysis of the solar and KamLAND data which rules out the standard oscillation scenario at 90% C.L, (ii) the measurement of the non-maximal value of θ_{23} by NO ν A which excludes the maximal mixing at 2.5σ C.L. and (iii) a discrepancy in the θ_{13} measurement by T2K which has a tension with the reactor best-fit value of $\sin^2 \theta_{13} = 0.021$ at 90% C.L. Our results show that all these three above mentioned anomalies can be explained if one assumes the existence of the non-standard interactions in neutrino propagation with $\theta_{23} = 45^\circ$ and $\sin^2 \theta_{13} = 0.021$ in the case of normal hierarchy. In our scenario the phase of $\epsilon_{e\tau}$ is zero and the most favorable value of the Dirac CP phase is approximately 255° .

PACS numbers: 14.60.Pq, 14.60.St, 26.65.+t

Neutrino oscillation experiments have been successful in determination of the three mixing angles (θ_{12} , θ_{13} and θ_{23}) and the two mass squared differences (Δm_{21}^2 and Δm_{31}^2). What remains to be studied is the mass hierarchy of neutrinos (either normal (NH): $\Delta m_{31}^2 > 0$ or inverted (IH): $\Delta m_{31}^2 < 0$), the precise value of the mixing angle θ_{23} and the Dirac CP phase δ_{CP} . There are many future experiments planned to determine these unknown quantities. In the mean time, a few tensions in neutrino experiments have been reported recently. They are: (i) the tension between the mass squared differences by the solar and KamLAND data [1] which gives a non-zero best-fit value of the non standard interaction parameters ϵ_D and ϵ_N . This rules out the standard oscillation scenario at 90% C.L, (ii) the tension between the T2K and NO ν A experiments regarding the measurement of the mixing angle θ_{23} [2, 3] and (iii) the tension in the measurement of the mixing angle θ_{13} by the reactor and T2K experiments [4, 5].¹ In Table. I we summarize the recent data of T2K and NO ν A. According to Ref. [4], T2K has observed a total of 28 events in the appearance channel and 120 events in the disappearance channel with a total POT (protons on target) of 6.6×10^{20} in the neutrino mode.² On the other hand NO ν A has seen 33 events in the appearance mode and 78 events in the disappearance mode with an exposure of 6.05×10^{20} POT in the neutrino mode [3]. From Table I, the tension between the T2K and NO ν A data are clearly visible. Regarding θ_{13} , T2K does its own fit and the best-fit value is much higher than reactor best fit which is $\sin^2 \theta_{13} = 0.021$. For θ_{23} , T2K data predicts maximal mixing. On the other hand NO ν A uses the reactor best-fit value for fitting and it excludes maximal mixing for θ_{23} at 2.5σ C.L. and gives a best-fit of $\sin^2 \theta_{23} = 0.4$.

In this Letter we look for a scenario which solves all these three tensions by introducing a flavor-dependent neutral current Non-Standard Interaction (NSI) in neutrino propagation [7–11]³. The purpose of our work is not to exhaust the whole parameter space but to show the existence of a new solution.

The NSI which we discuss here is described by the effective Lagrangian

$$\mathcal{L}_{\text{eff}}^{\text{NSI}} = -2\sqrt{2}\epsilon_{\alpha\beta}^{fP} G_F (\bar{\nu}_{\alpha L} \gamma_{\mu} \nu_{\beta L}) (\bar{f}_P \gamma^{\mu} f_P), \quad (1)$$

where f_P stands for fermions with chirality P and $\epsilon_{\alpha\beta}^{fP}$ is a dimensionless constant which is normalized by the Fermi coupling constant G_F . In the presence of this NSI, the neutrino evolution is governed by the Dirac equation:

$$i \frac{d}{dx} \begin{pmatrix} \nu_e(x) \\ \nu_{\mu}(x) \\ \nu_{\tau}(x) \end{pmatrix} = \left[U \text{diag} \left(0, \frac{\Delta m_{21}^2}{2E}, \frac{\Delta m_{31}^2}{2E} \right) U^{-1} + \mathcal{A} \right] \begin{pmatrix} \nu_e(x) \\ \nu_{\mu}(x) \\ \nu_{\tau}(x) \end{pmatrix}, \quad (2)$$

where

$$\mathcal{A} \equiv A \begin{pmatrix} 1 + \epsilon_{ee} & \epsilon_{e\mu} & \epsilon_{e\tau} \\ \epsilon_{\mu e} & \epsilon_{\mu\mu} & \epsilon_{\mu\tau} \\ \epsilon_{\tau e} & \epsilon_{\tau\mu} & \epsilon_{\tau\tau} \end{pmatrix}, \quad (3)$$

$A \equiv \sqrt{2}G_F N_e$, U is the leptonic mixing matrix, $\Delta m_{jk}^2 \equiv m_j^2 - m_k^2$, $\epsilon_{\alpha\beta}$ is defined by

$$\epsilon_{\alpha\beta} \equiv \sum_{f=e,u,d} \frac{N_f}{N_e} \epsilon_{\alpha\beta}^f. \quad (4)$$

¹ The latest measurement by Daya Bay [5] gives $\sin^2 \theta_{13} = 0.021$ and this lies within 90%CL of the T2K allowed region (See Fig. 31 of Ref. [4]). Although this may not be called a tension at present, if this trend persists as the statistics increases, the discrepancy between the mixing angles θ_{13} by the reactor and T2K experiments should be taken seriously in future.

² The recent update of the T2K data can be found in Ref. [6]. As the details of the fit are not available yet we take the latest published results for our analysis.

³ For recent studies of NSI in long-baseline experiments see [12].

Expt	$\sin^2 \theta_{13}$ NH (IH)	$\sin^2 \theta_{23}$ NH (IH)	δ_{CP} NH (IH)
T2K	0.0422 (0.0491)	0.524 (0.523)	1.91 (1.01)
NO ν A	0.021	0.040	1.49 π

TABLE I. Recent data of T2K and NO ν A .

We defined the new NSI parameters as $\epsilon_{\alpha\beta}^f \equiv \epsilon_{\alpha\beta}^{fL} + \epsilon_{\alpha\beta}^{fR}$ since the matter effect is sensitive only to the coherent scattering and only to the vector part in the interaction, and N_f ($f = e, u, d$) stands for the number densities of fermions f .

To discuss the effect of NSI on solar neutrinos, the 3×3 Hamiltonian in the Dirac equation Eq. (2) is reduced to an effective 2×2 Hamiltonian given by

$$H^{\text{eff}} = \frac{\Delta m_{21}^2}{4E} \begin{pmatrix} -\cos 2\theta_{12} & \sin 2\theta_{12} \\ \sin 2\theta_{12} & \cos 2\theta_{12} \end{pmatrix} + \begin{pmatrix} c_{13}^2 A & 0 \\ 0 & 0 \end{pmatrix} + A \sum_{f=e,u,d} \frac{N_f}{N_e} \begin{pmatrix} -\epsilon_D^f & \epsilon_N^f \\ \epsilon_N^{f*} & \epsilon_D^f \end{pmatrix}, \quad (5)$$

where ϵ_D^f and ϵ_N^f are linear combinations of the standard NSI parameters:

$$\epsilon_D^f = -\frac{c_{13}^2}{2} (\epsilon_{ee}^f - \epsilon_{\mu\mu}^f) + \frac{s_{23}^2 - s_{13}^2 c_{23}^2}{2} (\epsilon_{\tau\tau}^f - \epsilon_{\mu\mu}^f) + c_{13} s_{13} \text{Re} [e^{i\delta_{\text{CP}}} (s_{23} \epsilon_{e\mu}^f + c_{23} \epsilon_{e\tau}^f)] - (1 + s_{13}^2) c_{23} s_{23} \text{Re} [\epsilon_{\mu\tau}^f] \quad (6)$$

$$\epsilon_N^f = -c_{13} s_{23} \epsilon_{e\tau}^f + c_{13} c_{23} \epsilon_{e\mu}^f + s_{13} c_{23} s_{23} e^{-i\delta_{\text{CP}}} (\epsilon_{\tau\tau}^f - \epsilon_{\mu\mu}^f) + s_{13} e^{-i\delta_{\text{CP}}} (s_{23}^2 \epsilon_{\mu\tau}^f - c_{23}^2 \epsilon_{\mu\tau}^{f*}), \quad (7)$$

and $c_{jk} \equiv \cos \theta_{jk}$, $s_{jk} \equiv \sin \theta_{jk}$. In the analysis of Ref. [1], one particular choice of $f = u$ or $f = d$ was taken at a time because of the nontrivial composition profile of the Sun, and it was found that the best fit values are $(\epsilon_D^u, \epsilon_N^u) = (-0.22, -0.30)$ ($f = u$) or $(\epsilon_D^d, \epsilon_N^d) = (-0.12, -0.16)$ ($f = d$) from the solar neutrino and KamLAND data only, $(\epsilon_D^u, \epsilon_N^u) = (-0.140, -0.030)$ ($f = u$) or $(\epsilon_D^d, \epsilon_N^d) = (-0.145, -0.036)$ ($f = d$) from the global analysis of the neutrino oscillation data.

In this work we look for a scenario with NSI which gives a good fit to the solar and KamLAND data, the NO ν A data and the T2K data. For our analysis we use the GLoBES [13] and MonteCUBES [14] softwares. For our fit we will assume that the mixing angle θ_{23} in vacuum is maximal, i.e., $\theta_{23} = 45^\circ$ ⁴ and the mixing angle θ_{13} in vacuum is given by the reactor data, i.e., $\sin^2 \theta_{13} = 0.021$. We will do our analysis in the $(\epsilon_D^f, \epsilon_N^f)$ plane and for this we need to express $\epsilon_{\alpha\beta}$ as a function of $(\epsilon_D^f, \epsilon_N^f)$. So we proceed in the following way. As can

be seen from the definition of $\epsilon_{\alpha\beta}$, the neutrino oscillation experiments on the Earth are sensitive only to the sum of $\epsilon_{\alpha\beta}^f$. However, since the analysis of solar neutrinos was done either for $f = u$ or $f = d$ only, we also analyze the long baseline experiments assuming the same condition. Since the number of neutrons and that of electron is approximately equal in the Earth, if we turn on NSI for $f = u$ only or $f = d$ only, then from Eq. (4) we get

$$\epsilon_{\alpha\beta} = 3\epsilon_{\alpha\beta}^f. \quad (8)$$

As we can see from Eqs. (6) and (7), the mapping $\epsilon_{\alpha\beta}^f \rightarrow (\epsilon_D^f, \epsilon_N^f)$ is not one to one, and in general it is difficult to obtain the possible region for the $\epsilon_{\alpha\beta}$ parameters analytically. Here, instead of exhausting all the possible regions for $\epsilon_{\alpha\beta}$, we postulate the following:

$$\epsilon_D^f = -\frac{c_{13}^2}{2} (\epsilon_{ee}^f - \epsilon_{\mu\mu}^f) + \frac{s_{23}^2 - s_{13}^2 c_{23}^2}{2} (\epsilon_{\tau\tau}^f - \epsilon_{\mu\mu}^f) \quad (9)$$

$$0 = c_{13} s_{13} \text{Re} [e^{i\delta_{\text{CP}}} (s_{23} \epsilon_{e\mu}^f + c_{23} \epsilon_{e\tau}^f)] - (1 + s_{13}^2) c_{23} s_{23} \text{Re} [\epsilon_{\mu\tau}^f] \quad (10)$$

$$\epsilon_N^f = -c_{13} s_{23} \epsilon_{e\tau}^f \quad (11)$$

$$0 = c_{13} c_{23} \epsilon_{e\mu}^f + s_{13} c_{23} s_{23} e^{-i\delta_{\text{CP}}} (\epsilon_{\tau\tau}^f - \epsilon_{\mu\mu}^f) + s_{13} e^{-i\delta_{\text{CP}}} (s_{23}^2 \epsilon_{\mu\tau}^f - c_{23}^2 \epsilon_{\mu\tau}^{f*}), \quad (12)$$

Furthermore, for simplicity, we postulate $\text{Im} (s_{23}^2 \epsilon_{\mu\tau}^f - c_{23}^2 \epsilon_{\mu\tau}^{f*}) = 0$, which implies that $\epsilon_{\mu\tau}^f$ is a real parameter in the case of $\theta_{23} = 45^\circ$, and following the bound from the high energy atmospheric neutrino data, we take [16, 17]

$$\epsilon_{\tau\tau} = \frac{|\epsilon_{e\tau}|^2}{1 + \epsilon_{ee}}. \quad (13)$$

Another constraint comes from the atmospheric neutrino data, and the following must be satisfied: [18]

$$\left| \frac{\epsilon_{e\tau}}{1 + \epsilon_{ee}} \right| \lesssim 0.8 \quad \text{at } 2.5\sigma \text{CL}. \quad (14)$$

Finally, we put $\epsilon_{\mu\mu} = 0$ because we can always redefine $\epsilon_{ee} - \epsilon_{\mu\mu} \rightarrow \epsilon_{ee}$ and $\epsilon_{\tau\tau} - \epsilon_{\mu\mu} \rightarrow \epsilon_{\tau\tau}$. From these assumptions and Eqs. (8), (9), (10), (11), (12), (13) and (14), after putting $\theta_{23} = 45^\circ$, we get the following expressions:

$$\epsilon_{e\tau} = -\frac{3\sqrt{2}}{c_{13}} \epsilon_N^f \quad (15)$$

$$\epsilon_{ee} = -\frac{3}{c_{13}^2} \epsilon_D^f - \frac{1}{2} + \left\{ \left(\frac{3}{c_{13}^2} \epsilon_D^f - \frac{1}{2} \right)^2 + \frac{1}{c_{13}^2} |3\epsilon_N^f|^2 \right\}^{1/2} \quad (16)$$

$$\epsilon_{e\mu} = -\frac{s_{13}}{\sqrt{2} c_{13}} e^{-i\delta_{\text{CP}}} \frac{|\epsilon_{e\tau}|^2}{1 + \epsilon_{ee}} \quad (17)$$

$$\epsilon_{\mu\tau} = \frac{\sqrt{2}}{1 + s_{13}^2} c_{13} s_{13} \text{Re} [e^{i\delta_{\text{CP}}} (\epsilon_{e\mu} + \epsilon_{e\tau})] \quad (18)$$

Note that in all the best fit solutions from the solar+KamLAND analysis, both ϵ_D^f and ϵ_N^f have a phase (-1) , so in the present

⁴ A similar attempt was made in Ref. [15] to use NSI to reconcile the different values of θ_{23} for the neutrino and antineutrino modes.

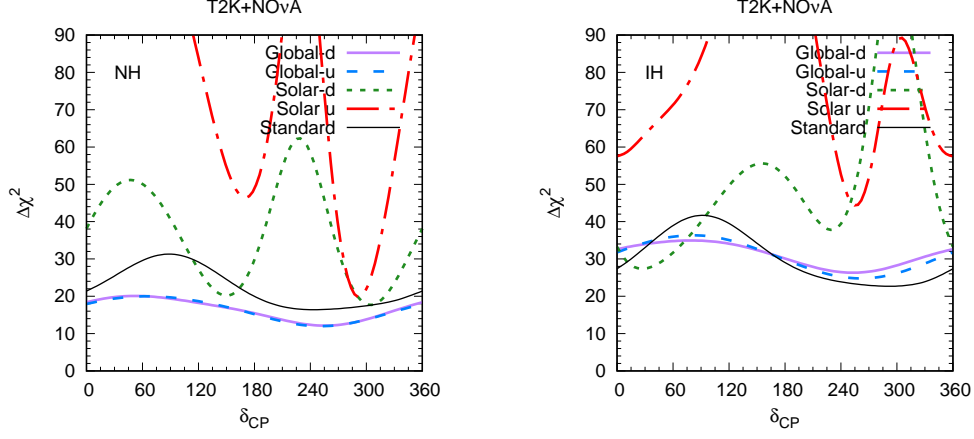


FIG. 1. The significance of the four best-fit solutions of the solar+KamLAND data (or the global analysis including the solar+KamLAND data; for $f = u$ or $f = d$) for the combined fit to the T2K and NO ν A data for NH (left panel) and IH (right panel). The black solid curve corresponds to the standard case with $\theta_{23} = 45^\circ$ and $\sin^2 \theta_{13} = 0.021$ without NSI.

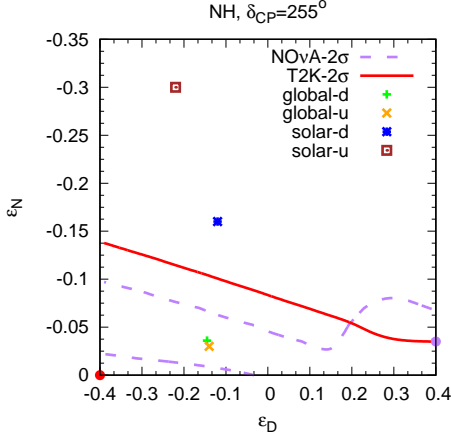


FIG. 2. Allowed region in the $\epsilon_D - \epsilon_N$ plane. The best-fit points for NO ν A and T2K are represented by the purple and red dot respectively.

ansatz we have $\arg(\epsilon_{e\tau})=0$ from Eq. (15), and $\arg(\epsilon_{e\mu}) = \pi - \delta_{CP}$ from Eq. (17).

Although our ansatz gives us only a special solution to Eqs. (6) and (7), it covers some of the whole solution space in the following way. We have verified that the appearance probability $P(\nu_\mu \rightarrow \nu_e)$ for NO ν A and T2K is not very sensitive to the small parameters $\epsilon_{e\mu}$ and $\epsilon_{\mu\tau}$. So even if we vary the $\epsilon_{\alpha\beta}$ in general, the behavior of the fit is not expected to be very much different from what is obtained by our ansatz.

Thus we obtained the values for the $\epsilon_{\alpha\beta}$ parameters which depend on one free parameter δ_{CP} . As we mentioned earlier there are four best-fit points (ϵ^{sol}) for the solar data. For our fit we calculated the χ^2 at each solar best-fit point for T2K and

NO ν A assuming $\theta_{23}^{fit} = 45^\circ$ and $\sin^2 \theta_{13}^{fit} = 0.021$ using the following formula:

$$\chi^2(\delta_{CP}) \equiv \sum_j \frac{1}{N_j^{data}} [N_j^{th}(\epsilon^{sol}, \theta_{23}^{fit}, \theta_{13}^{fit}) - N_j^{data}]^2, \quad (19)$$

where for ‘data’ we take the numbers as given in Table. I. In the analysis, we introduce the prior for $\epsilon_{e\mu}$ and $\epsilon_{\mu\tau}$:

$$\chi_{prior}^2 = 2.7 \left(\frac{|\epsilon_{e\mu}|}{0.15} \right)^2 + 2.7 \left(\frac{|\epsilon_{\mu\tau}|}{0.15} \right)^2, \quad (20)$$

where the bound for each parameter at 90%CL was taken from Ref. [19]. In the combined analysis, we evaluate the total χ^2 given by

$$\chi^2 = \chi_{nova}^2 + \chi_{T2K}^2 + \chi_{solar+KL}^2 + \chi_{prior}^2 \quad (21)$$

for all the values of δ_{CP} and plot in Fig. 1 for both the hierarchies. In Eq.(21) we approximated $\chi_{solar+KL}^2$ as $\chi_{solar+KL}^2 \simeq \chi^2(\epsilon_D) + \chi^2(\epsilon_N)$, where $\chi^2(\epsilon_D)$ and $\chi^2(\epsilon_N)$ are χ^2 obtained from the solar+KamLAND data in Ref. [1]. Obviously for the solar+KamLAND best-fit points, $\chi_{solar+KL}^2 = 0$, while for the global best-fit points, $\chi_{solar+KL}^2 = 0.1$. The latter was estimated from the Figure.2 of Ref. [1]. To estimate the goodness of fit, we compare our χ^2 with χ^2_{std} , i.e., the standard case. By χ^2_{std} we mean the value of χ^2 at $(\theta_{23}^{fit}, \theta_{13}^{fit})$ without NSI. Here the χ^2_{std} for solar+KamLAND is 3.8 (4.4) for $f = u$ ($f = d$), which is estimated by the approximation mentioned earlier. In our analysis we take the value $\chi_{solar+KL}^{2std} = 3.8$ for conservative estimation. On the other hand, the χ^2_{std} of T2K and NO ν A depend on δ_{CP} . For the standard case, therefore, we have $\chi_{nova}^{2std} + \chi_{T2K}^{2std} + 3.8$.

From Fig. 1 we see the following. For NH the two curves (solid-purple and dashed-blue) which correspond to the best-fit points of the global analysis of the solar data lie below the standard curve (solid-black) for all the values of δ_{CP} . This

ϵ_{ee}	$\epsilon_{e\tau}$	$\epsilon_{\tau\tau}$	$ \epsilon_{e\mu} $	$\epsilon_{\mu\tau}$
0.84885	0.12863	0.008950	0.00092689	-0.0067963

TABLE II. Values of $\epsilon_{\alpha\beta}$ corresponding to global- u best fit point of the solar data ($\epsilon_D = -0.14$, $\epsilon_N = -0.03$) at $\delta_{CP} = 255^\circ$.

implies that a nonstandard interaction at the solar best-fit point gives a better fit as compared to the standard case. Thus we found a new solution (the best-fit point of the global analysis of the solar+kamLAND data) with NSI which solves all the three neutrino tensions. Whereas in IH, a scenario with NSI in any region of δ_{CP} does not give χ^2 which is smaller than the minimum χ^2 in the standard case. From the plot we also see that in the case of NH, $\delta_{CP} \simeq 255^\circ$ is the most preferred value of δ_{CP} which gives the best fit with NSI. In Table II we give the values for $\epsilon_{\alpha\beta}$ corresponding to the global- u best-fit point of the solar data at $\delta_{CP} = 255^\circ$. For our information, in Fig. 2 we give the allowed region in the (ϵ_D, ϵ_N) plane for NO ν A and T2K at $\delta_{CP} = 255^\circ$ in the case of NH. As mentioned earlier, since ϵ_N^f ($\epsilon_{e\mu}$) has a phase (-1) (0) in all the best-fit solutions from the solar+kamLAND analysis, we performed our analysis only for $\epsilon_N^f < 0$. For the solar+kamLAND we give just the best-fit points. From these plots we identify the allowed region which is consistent with all the three anomalies under discussion. For NH we see that the global best-fit of the solar data is consistent with the NO ν A and T2K data within 2σ confidence regions.

In summary we found a scenario which explains the tension of the mass squared differences of the solar and KamLAND data, the one of mixing angles θ_{23} of the T2K and NO ν A data, and the discrepancy of θ_{13} of the reactor and T2K data. In our analysis we found that the goodness of fit for the NSI scenario is better for all the values of δ_{CP} in NH as compared to the standard case and that $\delta_{CP} \simeq 255^\circ$ give a bet-fit among others. For IH the NSI does not give a better fit. In this scenario, the three tensions give a constraint on the phase of $\epsilon_{e\tau}$ as zero and the most favorable value of the Dirac CP phase is $\simeq 255^\circ$. To be conclusive, we need more statistics of the T2K and NO ν A experiments. If the best fit values for θ_{23} at both the T2K and NO ν A experiments or the best fit values for θ_{13} of the reactor and T2K data remain the same as the statistics increases, then the present scenario with NSI will give a better fit to the data. It should be pointed out that the solar neutrino observation at the Hyperkamokande experiment is expected to test the tension between the solar and KamLAND data by the day night effect [20], and also that the atmospheric neutrino observation at the Hyperkamokande experiment is expected to test this NSI scenario by the matter effect in the multi-GeV energy range. [21]

Towards the completion of this work, we became aware of Ref. [22], which discussed part of the ideas in our paper from

a different point of view.

This research was partly supported by a Grant-in-Aid for Scientific Research of the Ministry of Education, Science and Culture, under Grants No. 25105009, No. 15K05058, No. 25105001 and No. 15K21734.

* Email Address: fukasawa-shinya@ed.tmu.ac.jp

† Email Address: monojit@tmu.ac.jp

‡ Email Address: yasuda@phys.se.tmu.ac.jp

- [1] M. C. Gonzalez-Garcia and M. Maltoni, JHEP **1309**, 152 (2013) [arXiv:1307.3092].
- [2] L. Magaletti, talk at NOW2016, Otranto, Italy, 4 – 11 September, 2016.
- [3] P. Vahle, talk at Neutrino 2016, 4-9 July, London.
- [4] K. Abe *et al.* [T2K Collaboration], Phys. Rev. D **91**, no. 7, 072010 (2015) [arXiv:1502.01550 [hep-ex]].
- [5] F. P. An *et al.* [Daya Bay Collaboration], Phys. Rev. Lett. **115**, no. 11, 111802 (2015) [arXiv:1505.03456 [hep-ex]].
- [6] H. A. Tanaka, talk at Neutrino 2016, 4-9 July, London.
- [7] L. Wolfenstein, Phys. Rev. D **17**, 2369 (1978).
- [8] M. M. Guzzo, A. Masiero and S. T. Petcov, Phys. Lett. B **260** (1991) 154.
- [9] E. Roulet, Phys. Rev. D **44**, R935 (1991).
- [10] T. Ohlsson, Rept. Prog. Phys. **76** (2013) 044201 [arXiv:1209.2710 [hep-ph]].
- [11] O. G. Miranda and H. Nunokawa, New J. Phys. **17** (2015) no.9, 095002 [arXiv:1505.06254 [hep-ph]].
- [12] M. Blennow, S. Choubey, T. Ohlsson, D. Pramanik and S. K. Raut, JHEP **1608**, 090 (2016) [arXiv:1606.08851 [hep-ph]], D. V. Forero and P. Huber, Phys. Rev. Lett. **117**, 031801 (2016) [arXiv:1601.03736 [hep-ph]], P. Coloma and T. Schwetz, Phys. Rev. D **94**, 055005 (2016) [arXiv:1604.05772 [hep-ph]], M. Masud, A. Chatterjee and P. Mehta, J. Phys. G **43**, no. 9, 095005 (2016) [arXiv:1510.08261 [hep-ph]], S. K. Agarwalla, S. S. Chatterjee and A. Palazzo, arXiv:1607.01745 [hep-ph], A. de Gouvêa and K. J. Kelly, Nucl. Phys. B **908**, 318 (2016) [arXiv:1511.05562 [hep-ph]].
- [13] P. Huber, M. Lindner and W. Winter, Comput. Phys. Commun. **167**, 195 (2005) [hep-ph/0407333].
- [14] M. Blennow and E. Fernandez-Martinez, Comput. Phys. Commun. **181**, 227 (2010) [arXiv:0903.3985 [hep-ph]].
- [15] O. Yasuda, AIP Conf. Proc. **1382**, 103 (2011) [arXiv:1012.3478 [hep-ph]].
- [16] A. Friedland, C. Lunardini and M. Maltoni, Phys. Rev. D **70**, 111301 (2004) [arXiv:hep-ph/0408264].
- [17] A. Friedland and C. Lunardini, Phys. Rev. D **72** (2005) 053009 [arXiv:hep-ph/0506143].
- [18] S. Fukasawa and O. Yasuda, Adv. High Energy Phys. **2015**, 820941 (2015) [arXiv:1503.08056 [hep-ph]].
- [19] C. Biggio, M. Blennow and E. Fernandez-Martinez, JHEP **0908**, 090 (2009) [arXiv:0907.0097 [hep-ph]].
- [20] T. Kajita, talk at NOW2016, Otranto, Italy, 4 – 11 September, 2016.
- [21] S. Fukasawa and O. Yasuda, arXiv:1608.05897 [hep-ph].
- [22] J. Liao, D. Marfatia and K. Whisnant, arXiv:1609.01786 [hep-ph].